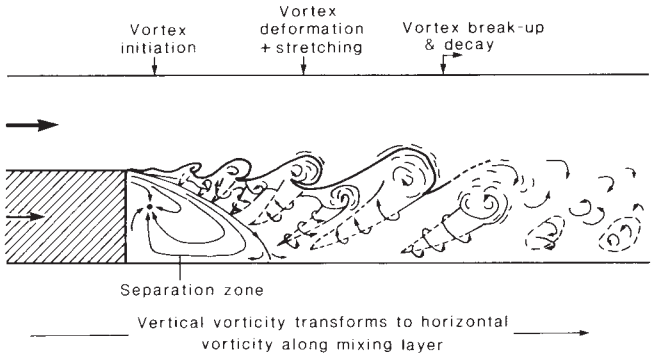

FIG. 3 A schematic model of mixing-layer distortion at the confluence of two flows of different depth. This planform diagram illustrates that deformation of the vertical mixing-layer vortices leads to the production of horizontal vorticity, enhanced mixing and fluid upwelling downstream of the confluence.

3). In Fig. 3 we illustrate a schematic model of this process of vortex and mixing-layer distortion.

Such complex three-dimensional deformation of the mixing layer is characteristic of all the unequal-depth mixing flows that we have studied. Although we have examined only zero degree confluence angles, mixing-layer distortion such as that described here can be expected at any junction in which the confluent channels are of different depths. The orientation of the separation zone is controlled by the planform geometry of the negative step, which in natural channels is formed by avalanche faces of tributary mouth bars which dip into the central confluence scour[1,5,6]. Consequently, the degree of entrainment of deeper-channel fluid into the separation zone and the position of the zone of upwelling will be dependent on the position of the tributary mouth bars, this itself being controlled by the junction angle and the ratio of discharges between the confluent channels[2,5,18]. This process of mixing-layer distortion and fluid upwelling may be invoked to explain patterns of fluid mixing at natural river junctions[22,23] where fluid from one channel is observed to upwell within the body of the other tributary flow downstream from the confluence.

The process we have outlined here has many implications. The dispersal of sediment at junctions across channel towards the shallower tributary may be greatly enhanced by such a depth differential between the confluent channels. This may influence erosion, through the position of the mixing layer and its associated higher Reynolds stresses, and deposition through control of the location of both zones of upwelling and the principal sediment transport pathways. Helical flow cells, which have been described at river channel confluences[1,20], may also originate from such depth-differential-controlled processes and not from any inherent helical flow where flows of equal depth combine. Attempts at modelling the near-field of side discharges in effluent dispersal[24] must also account for this mixing-layer distortion, which may significantly increase the potential for mixing across the shallower channel at a junction while simultaneously decreasing the rate of mixing across the deeper channel. Thus, effluents suspended in a deep channel may be rapidly transferred across the flow of a shallower channel when the two flows merge. □

Received 19 November 1990; accepted 18 February 1991.

1. Mosley, M. P. *J. Geol.* **84,** 535–562 (1976).
2. Ashmore, P. E. & Parker, G. *Water Resour. Res.* **19,** 342–402 (1983).
3. Roy, A. G. & Bergeron, N. *Geomorphology* **3,** 99–112 (1990).
4. Klassen, G. J. & Vermeer, K. *Proc. Int. Conf. Fluvial Hydraul.* Budapest, 1–14 (1988).
5. Best, J. L. *Sedimentology* **35,** 481–498 (1988).
6. Mosley, M. P. & Schumm, S. A. *Econ. Geol.* **72,** 691–694 (1977).
7. Reid, I., Best, J. L. & Frostick, L. E. in *Floods: Hydrological, Sedimentological and Geomorphological Implications* (eds Beven, K. & Carling, P.) 135–150 (Wiley, Chichester, 1989).
8. Bryant, I. D., Holyoak, D. T. & Mosely, K. A. *Proc. Geol. Ass.* **94(4),** 321–343 (1983).
9. Best, J. L. & Brayshaw, A. C. *J. geol. Soc. Lond.* **142,** 747–755 (1985).
10. Soong, H. K. thesis, Univ. Connecticut (1976).
11. Hager, W. H. *J. hydraul. Engng* **115,** 243–259 (1989).
12. Sutherland, A. J. in *Proc. 9th Aus. Fluid Mech. Conf.* 259–263 (Univ. of Auckland, 1986).
13. Chu, V. H. & Babarutsi, S. *J. hydraul. Engng* **114,** 1257–1274 (1988).
14. Richards, K. S. *Water Resour. Res.* **16,** 241–244 (1980).
15. Best, J. L. & Reid, I. *J. hydraul. Engng* **110,** 1588–1594 (1984).
16. Roy, A. G. & Woldenberg, M. J. *J. Geol.* **94,** 401–411 (1986).
17. Roy, A. G. & Roy, R. *Earth Surf. Proc. Landf.* **13,** 77–84 (1988).
18. Best, J. L. *Soc. Econ. Palaeontalogists and Mineralogists spec. Publ.* **39,** 27–35 (1987).
19. Kennedy, B. A. *Earth Surf. Proc. Landf.* **9,** 153–173 (1984).
20. Ashmore, P. E. *Earth Surf. Proc. Landf.* **7,** 201–225 (1982).
21. Winant, C. D. & Browand, F. K. *J. Fluid Mech.* **63,** 237–255 (1974).
22. Sternberg, H. O. *The Amazon River of Brazil* 74 (Steiner, Weisbader, 1975).
23. Roy, A. G. & De Serres, B. *Bull. Soc. Géog. Liège* **25,** 113–127 (1989).
24. McGuirk, J. J. & Rodi, W. *J. Fluid Mech.* **86,** 761–781 (1978).

ACKNOWLEDGEMENTS. We thank the Earth Sciences workshop at Leeds for construction of the mixing-flow apparatus. Travel for A.G.R. was made possible through a grant from FCAR; this paper was prepared while J.L.B. held a Royal Society/NSERC Anglo-Canadian Scientific Exchange Scheme Fellowship at the Université de Montréal that was also supported by the Foundation for Canadian Studies. We are grateful for the thoughtful comments of Jim Pizzuto.

Microbial reduction of uranium

Derek R. Lovley, Elizabeth J. P. Phillips, Yuri A. Gorby & Edward R. Landa

Water Resources Division, 430 National Center, US Geological Survey, Reston, Virginia 22092, USA

REDUCTION of the soluble, oxidized form of uranium, U(VI), to insoluble U(IV) is an important mechanism for the immobilization of uranium in aquatic sediments and for the formation of some uranium ores[1–10]. U(VI) reduction has generally been regarded as an abiological reaction in which sulphide, molecular hydrogen or organic compounds function as the reductant[1,2,5,11]. Microbial involvement in U(VI) reduction has been considered to be limited to indirect effects, such as microbial metabolism providing the reduced compounds for abiological U(VI) reduction and microbial cell walls providing a surface to stimulate abiological U(VI) reduction[1,12,13]. We report here, however, that dissimilatory Fe(III)-reducing microorganisms can obtain energy for growth by electron transport to U(VI). This novel form of microbial metabolism can be much faster than commonly cited abiological mechanisms for U(VI) reduction. Not only do these findings expand the known potential terminal electron acceptors for microbial energy transduction, they offer a likely explanation for the deposition of uranium in aquatic sediments and aquifers, and suggest a method for biological remediation of environments contaminated with uranium.

It is becoming increasingly clear that the reduction of metals in anaerobic environments is often the result of the direct enzymatic reduction by bacteria[14,15]. For example, the Fe(III)-reducing microorganism, strain GS-15, grows under anaerobic conditions by enzymatically coupling the oxidation of acetate to carbon dioxide with the reduction of Fe(III) to Fe(II)[16,17] according to:

$$CH_3COO^- + 8Fe(III) + 4H_2O \rightarrow 8Fe(II) + 2HCO_3^- + 9H^+$$

Thermodynamic calculations have indicated that, per electron transferred, acetate oxidation coupled to U(VI) reduction has the potential to yield more than twice the energy that is available from Fe(III) reduction[8]. When GS-15, grown on acetate and Fe(III), was inoculated into an anaerobic medium with acetate as the sole electron donor and U(VI) as the potential electron acceptor, U(VI) was reduced to U(IV) over time (Fig. 1*a*). Growth coincided with U(VI) reduction and stopped as U(VI) became depleted. When [2-^{14}C]-acetate was incorporated into the medium, $^{14}CO_2$ was generated in direct proportion to U(VI) reduction (Fig. 1*b*). In a separate experiment in which acetate concentrations were measured in cultures growing with U(VI) reduction, U(VI) and acetate loss over time were linearly related (correlation coefficient $r = 0.9$) with a U(VI)/acetate ratio of

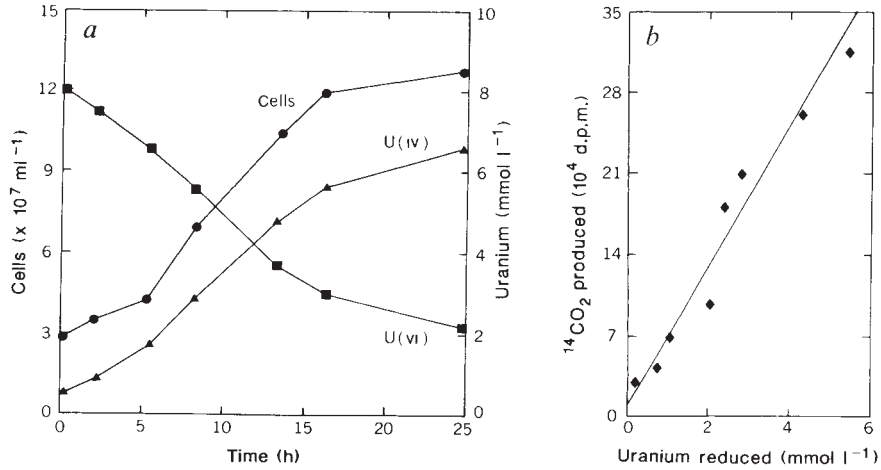

FIG. 1 Cell numbers, and U(VI) and U(IV) concentrations over time (*a*), and relationship between $^{14}CO_2$ production from [2-^{14}C]-acetate and U(VI) reduction (*b*) when GS-15 was inoculated into a medium with acetate as the electron donor and U(VI) as the electron acceptor. GS-15 obtained energy to support growth by reducing U(VI) to U(IV) while oxidizing acetate to carbon dioxide.
METHODS. Cells grown anaerobically at 30 °C in an acetate-Fe(III)-citrate medium[17] were inoculated into a similar medium but with Fe(III) replaced with 10 mmol l^{-1} uranyl chloride. Acetate concentrations were: 10 mmol l^{-1} (*a*) and 3.5 mmol l^{-1} (including 0.5 μCi of [2-^{14}C]-acetate (53 mCi/mmol)) (*b*). Cell numbers[17] and $^{14}CO_2$ produced[29] were determined as previously described. All manipulations for the determination of U(VI) and U(IV) concentrations were carried out in an anaerobic chamber. Subsamples were acidified with 1.2 N HCL to provide a final concentration of 4 N HCL. In (*a*), 2 ml of each acidified subsample were immediately added to a glass column (10-cm length, 1-cm inner diameter) containing Dowex AG1X8. As previously determined[8], on this column U(VI) is retained in 4 N HCl whereas U(IV) is not. The column was washed with 20 ml of 4 N HCL to collect the U(IV) and then washed with 20 ml of 0.1 N HCL to elute the U(VI). The concentrations of uranium in the U(VI) and U(IV) fractions were determined by directly aspirating the samples into a directly coupled plasma spectrometer and monitoring absorption at 424.167 nm. In (*b*), U(VI) in the anaerobic, acidified samples was analysed with a kinetic phosphorescence analyser (KPA-10, Chemchek Instruments), which uses a pulsed nitrogen dye laser and a complexing agent to measure U(VI) in solution. The loss of U(VI) as measured by this method could be accounted for by the production of U(IV) when samples were also analysed by the method used in (*a*).

3.6:1. Given that a small proportion of the acetate metabolized would be incorporated into cells, these results indicate that GS-15 can obtain energy for growth by oxidizing acetate with the reduction of U(VI) to U(IV) according to:

$$CH_3COO^- + 4U(VI) + 4H_2O \rightarrow 4U(IV) + 2HCO_3^- + 9H^+$$

Energy conservation from acetate oxidation coupled to U(VI) reduction should be through electron-transport and oxidative phosphorylation, because there is no known mechanism to generate net ATP through substrate level phosphorylation with acetate as the substrate. Subsequent studies have indicated that, in GS-15, electron transport to U(VI) proceeds through a respiratory chain containing cytochrome b_{558} (Y.G., manuscript in preparation). GS-15 is considered to reduce U(VI) directly rather than indirectly through reduction of Fe(III) with subsequent reduction of U(VI) by Fe(II), because Fe(II) did not reduce U(VI) in the growth medium and U(VI) was rapidly reduced in cell suspensions that had been repeatedly washed and resuspended in iron-free buffer.

One other organism, *Alteromonas putrefaciens*, is known to obtain energy for growth from electron transport to Fe(III)[18,19]. *A. putrefaciens* grew with H_2 as the sole electron donor and U(VI) as the electron acceptor (Fig. 2). In parallel studies, the stoichiometry of H_2 consumption and U(VI) reduction was consistent with the reaction:

$$H_2 + U(VI) \rightarrow U(IV) + 2H^+$$

Other electron donors for Fe(III) reduction by *A. putrefaciens* (formate, lactate, pyruvate) also supported U(VI) reduction.

Neither H_2 nor any of the organic electron donors for U(VI) reduction by GS-15 or *A. putrefaciens* reduced U(VI) in the absence of the organisms (Fig. 3 and data not shown). Furthermore, reduction of U(VI) in washed cell suspensions of GS-15 or *A. putrefaciens* was much faster than the reduction of U(VI) in the presence of a high concentration (1 mmol l^{-1}) of sulphide (Fig. 3). With extended incubation, cell suspensions of GS-15 reduced U(VI) concentrations below 0.4 μmol l^{-1}.

These results demonstrate that, although abiological reduction of U(VI) by sulphide, H_2 or organic compounds is typically considered to be the mechanism for U(VI) reduction in sedimentary environments[1,2,5,11], enzymatic reduction of U(VI) by microorganisms using U(VI) as a terminal electron acceptor is also possible. Furthermore, microbial reduction of U(VI) has the potential to proceed much more rapidly than abiological U(VI) reduction. Previous evidence for the potential of microorganisms to reduce U(VI) was the report that, in the presence of U(VI), crude cell-free extracts of *Micrococcus lactilyticus* consumed H_2 in quantities that were consistent with U(VI) reduction to U(IV)[20]. But these extracts reduced a wide range of metals with no evidence that the metal reduction was an enzymatic reaction or had any physiological significance in whole cells[15].

To evaluate more fully the relative potential for microbiological and abiological U(VI) reduction in reduced sediments, U(VI) was added to highly reduced methane-producing, sulphide-containing sediments of the Potomac River (Fig. 4). U(VI) reduction was much more rapid and extensive in the biologically

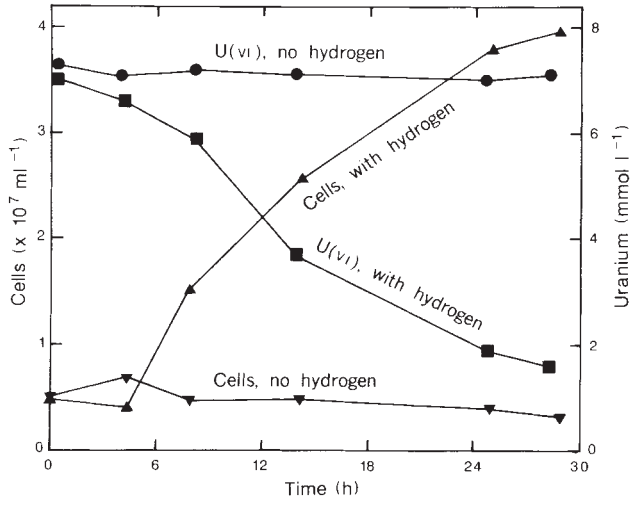

FIG. 2 Cell numbers and U(VI) and U(IV) concentrations over time when *Alteromonas putrefaciens* was inoculated into a U(VI)-containing medium with or without H_2. *A. putrefaciens* grew with the reduction of U(VI) to U(IV) in the presence of H_2, but not with H_2 omitted.
METHODS. Cells grown anaerobically at 30 °C with H_2 (60 kPa) as the electron donor and Fe(III)-citrate as the electron acceptor[18] were inoculated into a similar medium but with Fe(III) replaced with 10 mmol l^{-1} uranyl acetate. Controls had no added H_2. U(VI) was determined as in Fig. 1*b*.

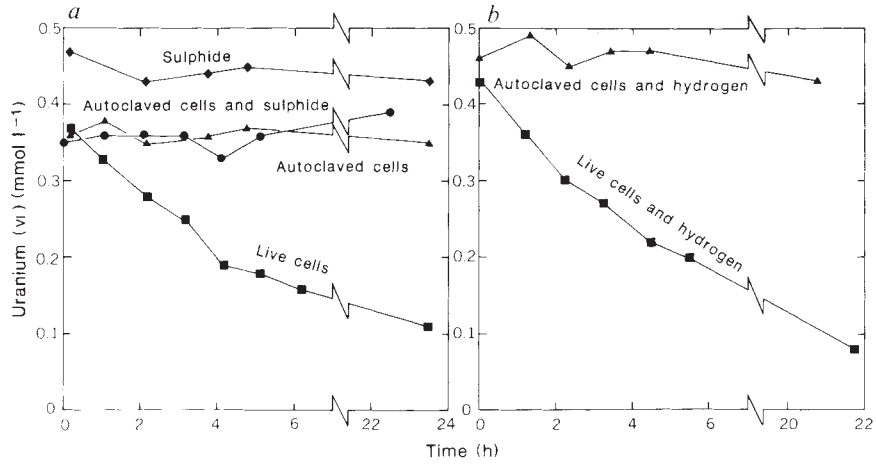

FIG. 3 U(VI) concentrations over time in the presence of various combinations of potential U(VI) reductants and cells of GS-15 (*a*) or *Alteromonas putrefaciens* (*b*). U(VI) was only reduced in the presence of actively metabolizing cells.
METHODS. Washed cells of Fe(III)-grown GS-15 (*a*) or *A. putrefaciens* (*b*) were suspended at 30 °C under N_2-CO_2 (80:20) in 10 ml of bicarbonate buffer ($NaHCO_3$, 0.025g; pH 6.7) containing uranyl acetate (0.4 mmol l^{-1}) to provide ~100 ng of cell protein per ml. Sodium sulphide (1 mmol l^{-1}) or H_2 (56 kPa) were added as noted. Aliquots were removed over time, flushed with N_2-CO_2 to remove sulphide if necessary, and U(VI) was determined as in Fig. 1*b*.

active sediments than in sediments in which the microorganisms were inactivated with heat. The microorganisms responsible for the U(VI) reduction were not identified, but these sediments do contain Fe(III)-reducing microorganisms which rapidly become active when an electron acceptor is added[21]. These results further suggest that models for U(IV) deposition in sedimentary environments should consider the possibility that microbial populations that have grown up with Fe(III), or possibly other electron acceptors, can reduce U(VI) entering these environments.

Geochemical evidence from a number of environments is consistent with U(VI) reduction by Fe(III)-reducing microorganisms leading to U(IV) deposition. For example, in marine sediments, deposition of U(IV) typically takes place within the sediment zone in which microorganisms oxidize organic matter with the reduction of Fe(III)[4-8,10]. Sulphide is unlikely to be the U(VI) reductant in these instances as sulphide does not accumulate in the Fe(III)-reducing zone of marine sediments. Furthermore, sulphide does not appear to reduce U(VI) in marine waters[9,22,23]. Abiological reduction of U(VI) by organic matter or H_2 in the Fe(III)-reducing zone of sediments also seems unlikely because organic-matter reduction of U(VI) is restricted to high temperature (>120 °C)[24,25] and, as shown above, at low temperatures, H_2 does not readily reduce U(VI) in the absence of microbial activity.

The common observation of U(IV) accumulations in the bleached 'reduction spots' of otherwise red, Fe(III)-rich rocks[26,27] provides another example in which uranium deposition is likely to be associated with the activity of Fe(III)-reducing bacteria. The lack of red colour in the reduction spots is due to localized reduction of Fe(III) which, recent evidence suggests, is the result of microbial Fe(III) reduction[26,28]. Even for environments such as sandstone- or roll-type uranium deposits, in which there is a co-accumulation of sulphide and U(IV) minerals, there is no direct evidence for sulphide reduction of U(VI) and other reduction mechanisms cannot be ruled out[12].

The potential for uranium contamination of surface and ground waters through uranium mining activities, irrigation of agricultural lands and disposal of nuclear wastes is an environmental concern. The results presented here suggest that, in many instances, it may be possible to immobilize uranium contamination by stimulating microbial U(VI) reduction in aquatic sediments or ground water. GS-15 and other Fe(III)-reducing microorganisms can oxidize important organic contaminants with Fe(III) as the electron acceptor[29,30]. Thus, in the case of 'mixed wastes', which contain both organic contaminants and radioactive metals, the activity of U(VI)-reducing bacteria might be able to couple the decomposition of toxic organic compounds with the immobilization of uranium. Other radioactive metals, such as plutonium and technetium, which have multiple redox states and are insoluble in the reduced form, could potentially be treated in a similar manner. □

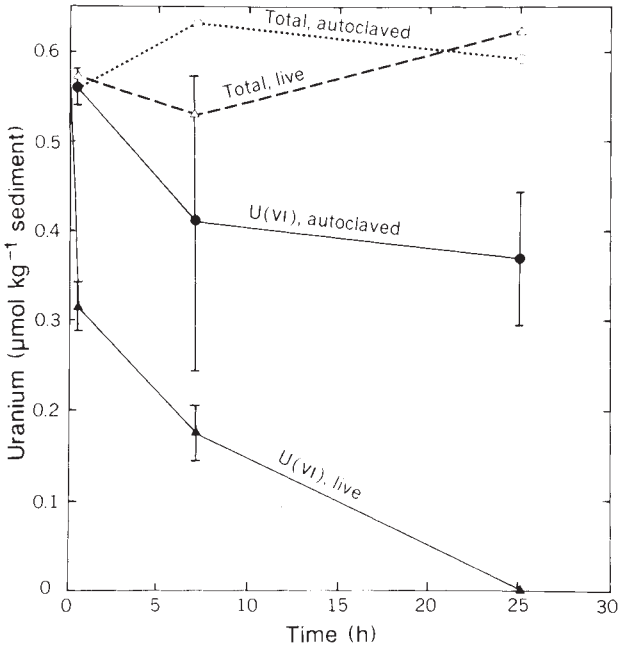

FIG. 4 Concentrations of U(VI) and total uranium over time in live and sterilized sediments. U(VI) was reduced much faster and more completely in live sediments, which reduced U(VI) below the detection limit of 2 nmol l^{-1} within 25 h.
METHODS. Uranyl acetate was added to anaerobically incubated, methane-producing sediments from the Potomac River in which sulphate had already been reduced to sulphide[21]. Sediments were autoclaved four times (121 °C, 1 h) for abiotic controls. Over time, subsamples (~0.3 g) were removed and extracted under anaerobic conditions in 5 ml of 100 mmol l^{-1} bicarbonate for 30 min. U(VI) was measured as in Fig. 1*b*. To determine total uranium in the extracts, U(IV) was first oxidized to U(VI) by bubbling the extract in air for 5 min.

Received 8 November 1990; accepted 15 January 1991.

1. Jensen, M. L. *Econ. Geol.* **53,** 598-616 (1958).
2. Hostetler, P. B. & Garrels, R. M. *Econ. Geol.* **57,** 137-167 (1962).
3. Turekian, K. K. & Bertine, K. K. *Nature* **229,** 250-251 (1971).
4. Bonatti, E., Fisher, D. E., Joensuu, O. & Rydell, H. S. *Geochim. cosmochim. Acta* **35,** 189-201 (1971).
5. Langmuir, D. *Geochim. cosmochim. Acta* **42,** 547-569 (1978).
6. Kadko, D. *Earth planet. Sci. Lett.* **51,** 115-131 (1980).
7. Colley, S. & Thomson, J. *Geochim. cosmochim. Acta* **49,** 2339-2348 (1985).
8. Cochran, J. K., Carey, A. E., Sholkovitz, E. R. & Surprenant, L. D. *Geochim. cosmochim. Acta* **50,** 663-680 (1986).
9. Anderson, R. F., LeHuray, A. P., Fleisher, M. Q. & Murray, J. W. *Geochim. cosmochim. Acta* **53,** 2205-2213 (1989).
10. Wallace, H. E. *et al. Geochim. cosmochim. Acta* **52,** 1557-1569 (1988).
11. Maynard, J. B. *Geochemistry of Sedimentary Ore Deposits* (Springer, New York, 1983).

12. Taylor, G. H. in *Biogeochemical Cycling of Mineral-Forming Elements* (eds Trudinger, P. A. & Swaine, D. J.) 485–514 (Elsevier, New York, 1979).
13. Mohagheghi, A., Updegraff, D. M. & Goldhaber, M. B. *Geomicrobiol. J.* **4,** 153–173 (1985).
14. Ehrlich, H. L. *Geomicrobiology* (Marcel Dekker, New York, 1990).
15. Ghiorse, W. C. in *Biology of Anaerobic Microorganisms* (ed. Zehnder, A. J. B.) 305–331 (Wiley, New York, 1988).
16. Lovley, D. R., Stolz, J. F., Nord, G. L. & Phillips, E. J. P. *Nature* **330,** 252–254 (1987).
17. Lovley, D. R. & Phillips, E. J. P. *Appl. environ. Microbiol.* **54,** 1471–1480 (1988).
18. Lovley, D. R., Phillips, E. J. P. & Lonergan, D. J. *Appl. environ. Microbiol.* **55,** 700–706 (1989).
19. Myers, C. R. & Nealson, K. H. *Science* **240,** 1319–1321 (1988).
20. Woolfolk, C. A. & Whiteley, H. R. *J. Bacteriol.* **84,** 647–658 (1962).
21. Lovley, D. R. & Phillips, E. J. P. *Appl. environ. Microbiol.* **53,** 2636–2641 (1987).
22. Anderson, R. F., Fleisher, M. Q. & LeHuray, A. P. *Geochim. cosmochim. Acta* **53,** 2215–2224 (1989).
23. Anderson, R. F. *Uranium* **3,** 145–164 (1987).
24. Breger, I. A. in *Formation of Uranium Ore Deposits* 99–124 (International Atomic Energy Agency, Vienna, 1974).
25. Nakashima, S., Disnar, J. R., Perruchot, A. & Trichet, J. *Geochim. cosmochim. Acta* **48,** 2321–2329 (1984).
26. Hoffman, B. A. *Chem. Geol.* **81,** 55–81 (1990).
27. Harrison, R. K. *G.B. geol. Surv. Bull.* **52,** 1–26 (1975).
28. Lovley, D. R., Chapelle, F. H. & Phillips, E. J. P. *Geology* **18,** 954–957 (1990).
29. Lovley, D. R. *et al. Nature* **339,** 297–299 (1989).
30. Lovley, D. R. & Lonergan, D. J. *Appl. environ. Microbiol.* **56,** 1858–1864 (1990).

ACKNOWLEDGEMENTS. We thank Ruth Smith and Ray Van Hoven for technical assistance and Ron Oremland, Tom Kraemer, Marty Goldhaber, Rich Reynolds and Richard Smith for helpful discussions. This study was supported by the US Geological Survey Toxic Waste/Groundwater Contamination Programme.

Evidence for volcanic eruption on the southern Juan de Fuca ridge between 1981 and 1987

William W. Chadwick Jr*, Robert W. Embley† & Christopher G. Fox†

* OSU/CIMRS, Hatfield Marine Science Center, Newport, Oregon 97365, USA
† PMEL/NOAA, Hatfield Marine Science Center, Newport, Oregon 97365, USA

THE formation of new ocean crust at mid-ocean ridges is known to be a discontinuous process in both space and time, but little is known about the frequency and duration of eruptions along an active ridge segment. Here we present evidence, from Sea Beam surveys and underwater photography, for the eruption of lavas along a segment of the Juan de Fuca ridge between 1981 and 1987. Although previous studies have inferred volcanic activity on ridges in areas where recent seismicity or young lava flows have been observed[1–4], none has yet had direct evidence to date such a recent submarine eruption. The temporal coincidence between this eruptive episode and the megaplumes (huge, sudden emissions of hot mineral-laden water) observed over this part of the ridge[5,6] in 1986 and 1987 supports previous suggestions[5–10] that megaplumes are caused by sea-floor spreading events.

The lavas that were erupted during the 1980s occur as a series of pillow mounds and ridges between 45°00.5′ N and 45°09.5′ N along the northern Cleft segment (Fig. 1). The evidence for the recent eruption of these lavas was first discovered through a discrepancy between microbathymetry derived from a towed camera system and bathymetric charts based on Sea Beam surveys. Three camera tows (collected in 1989 from the National Oceanic Atmospheric Administration (NOAA) ship *Discoverer*) over the southernmost pillow mound (mound 1, Fig. 1) showed glassy lava flows forming a 35-m-high hill, ~1 km in diameter. Earlier Sea Beam bathymetry (based on data collected in May 1981 from the NOAA ship *Surveyor*) shows no such hill, but instead a gentle slope to the east (Fig. 2*a*). The Sea Beam and camera-tow bathymetry correspond closely in other areas.

Other surveys confirm the recent appearance of mound 1. Bathymetry from Sea Beam surveys conducted over the same area by the research vessel *Atlantis II* in September 1987 and by the *Discoverer* in August 1990 shows a 25-m-high mound in the exact location of the glassy lavas delineated by the camera tows (Fig. 2*b*). Mound 1 was also imaged by a SeaMARC I sidescan survey in August 1987 from the *Discoverer*, and appears as an unfractured positive relief feature which covers pre-existing fractures (Fig. 3). The date of eruption of mound 1 is further restricted by a single Sea Beam swath collected during a camera tow by the *Surveyor* in June 1983. Although the data only sample the western edge of mound 1, the coverage is adequate to show that the 1983 swath has the same pre-eruption depth contours as the 1981 Sea Beam survey, and does not show the contours of the new lava mound. These Sea Beam surveys definitely constrain the time of the eruption of mound 1 to between 1981–1987, and probably to between 1983–1987.

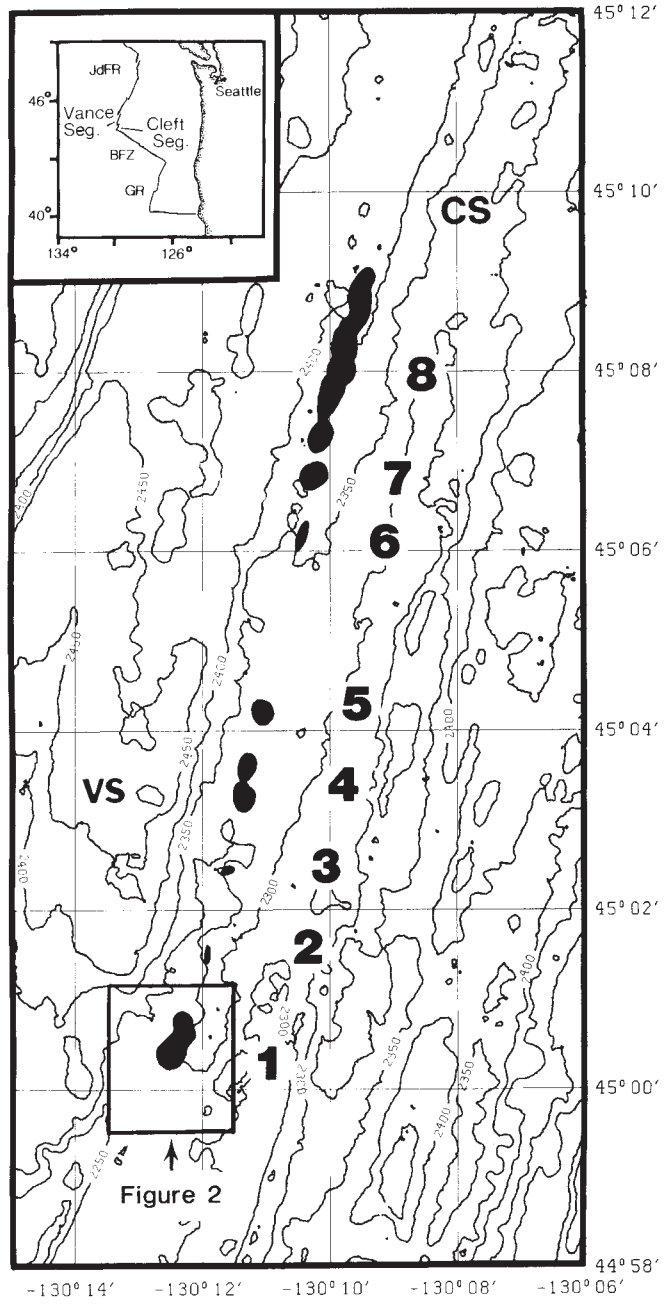

FIG. 1 Sea Beam bathymetric map of overlap region between Cleft and Vance segments, southern Juan de Fuca ridge (50-m contours); CS is northern end of Cleft segment, VS is southern end of Vance segment. Solid black areas show locations of new pillow lava mounds. Numbers to right of each mound are for identification in text. Box around mound 1 shows outline of Fig. 2. On inset map, GR is Gorda ridge, BFZ is Blanco Fracture Zone, and JdFR is Juan de Fuca ridge.